

CFD MODELING FOR DESIGN OF NO_x CONTROL SYSTEMS IN TWO UTILITY BOILERS

James Valentine, Marc Cremer, and Kevin Davis
Reaction Engineering International

J. J. Letcatvits
American Electric Power

Scott Vierstra
Savvy Engineering

ABSTRACT

A two-phase, reacting flow CFD code was used in the design and evaluation of NO_x control strategies for two pulverized coal utility boilers. The effects of furnace staging, burner alterations, and water injection were assessed in these furnaces. CFD analysis was shown to be a useful tool in optimizing NO_x reduction while minimizing adverse effects such as increases in furnace CO emission and carbon in fly ash.

The first boiler evaluated was a 265 MW B&W subcritical, opposed-wall fired, unstaged furnace. Furnace CFD simulations identified locations of highest flue gas mass flows and highest CO and O₂ concentrations and were used to identify OFA port locations for maximum NO_x reduction. Simulations of an OFA and burner alteration configuration that has been subsequently installed predicted a 34% reduction in NO_x emission with minimal changes in furnace exit CO and unburned carbon in fly ash. Plant CEMS data confirmed the accuracy of the modeling results for both the pre-retrofit and the post-retrofit operations

The second furnace analyzed was a 153 MW B&W subcritical, roof-fired furnace. This furnace is equipped with 10 multi-tip burners and 10 NO_x ports located below the burners. A CFD analysis predicted that a 23% decrease in NO_x emission with little adverse effect on furnace exit CO or carbon in fly ash was achievable through a combination of deeper staging and burner alterations. Further CFD analysis identified high NO_x production zones in the downstream part of the combustion zone. It was predicted that selectively attacking these regions with water injection could further lower furnace NO_x emission to a level 37% below the current baseline operating condition. In designing an effective water injection such as this, it is crucial that NO_x production zones in the downstream portion combustion field be identified, since these regions are most likely to produce NO_x that will not be reduced before exiting the furnace.

INTRODUCTION

The electric utility industry is facing aggressive NO_x reduction requirements in coal fired furnaces. Proven NO_x control technologies are available that provide a range of performance over a range of operating and capital costs. Selective Catalytic Reduction (SCR) has been proven in Europe and Asia to reliably achieve 75-85% NO_x reduction in coal fired units. However, these reductions come at high capital and operating cost. In certain existing units, the installation and operation of SCR is cost prohibitive. As a result, utilities are interested in

evaluation of other lower cost technologies for certain units that can still achieve compliance over the fleet.

Recently CFD modeling has found increasing use in the design and evaluation of utility boiler retrofits, combustion optimization, and NO_x reduction technologies. For example, over the past eight years Reaction Engineering International (REI) has performed CFD modeling using in-house software for over 100 fossil-fuel fired utility boilers to evaluate the performance and impact of NO_x reduction technologies such as staging and overfire air, low NO_x burners, visciated air and air preheating, flue gas recirculation, co-firing of opportunity fuels, fuel blending, Rich Reagent Injection (RRI), Selective Non-catalytic Reduction (SNCR), gas reburning, and Fuel Lean Gas Reburning (FLGR). Boilers have ranged in size from 34 MW to 1300 MW and include cyclone, tangential, wall, and roof fired systems. Figure 1 shows the unit size distribution of cyclone, tangential and wall-fired units modeled by REI over the past eight years. The large majority of these units were coal-fired, requiring modeling software capable of accounting for the turbulent two-phase mixing, equilibrium (e.g., CO₂, O₂) and finite-rate (e.g., NO_x) gas-phase chemical reactions, heterogeneous coal particle reactions (devolatilization and char oxidation), and radiant and convective heat transfer that comprise combustion processes.

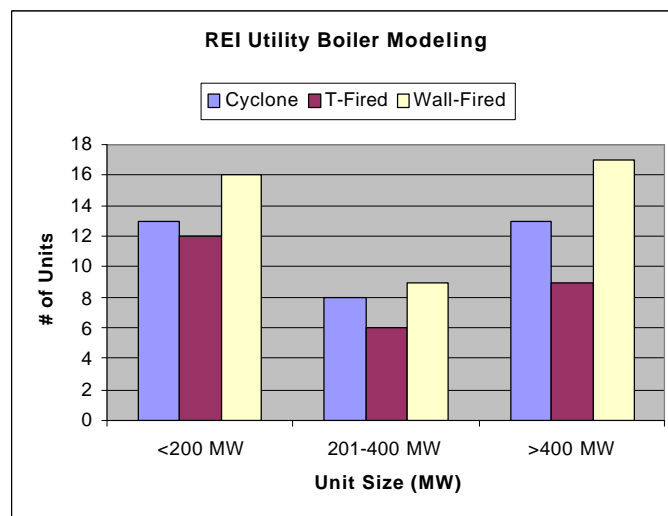


Figure 1. Distribution of utility boilers modeled by REI.

AEP Service Corporation has had significant experience in the design and installation of over 30 NO_x reduction retrofits in various types of coal fired furnaces. These NO_x reduction systems include OFA, burner alteration, and water injection schemes. AEP Service Corporation has found CFD analysis to be an effective tool in the design of many of these NO_x reduction systems.

In the hands of experienced combustion and CFD engineers, CFD modeling provides a valuable tool to evaluate impacts of potential burner and furnace alterations on NO_x emissions, as well as unburned carbon in fly ash, CO emissions and waterwall corrosion. It is particularly useful in the evaluation of “one-of-a-kind” systems in which the experience base is limited. This paper describes how CFD modeling has been utilized to evaluate and design cost effective NO_x

reduction strategies in a 265 MW B&W opposed wall-fired pc furnace and a 150 MW B&W roof-fired pc furnace.

APPROACH

The evaluations described here required the construction of a CFD model description of the modeled units under “baseline” operation representative of typical full load operating conditions. The CFD results were verified by comparison with unit performance including NO_x and CO emissions and carbon in ash. Parametric simulations were then completed to evaluate impacts of burner alterations, deeper staging, and in the case of the roof-fired unit, water injection. The simulations were carried out in series so that simulation results could be utilized to make incremental improvements to the designs. Based on the results of all simulations, specific designs were proposed for installation. The following sections describe the modeling in additional detail. A description of the CFD model is first provided, followed by a discussion of the approach used to develop a CFD model of these units.

CFD MODEL

The REI combustion models (Bockelie et al, 1998) employ a combination of Eulerian and Lagrangian reference frames. The flow field is assumed to be a steady-state, turbulent, reacting continuum field that can be described locally by general conservation equations. The governing equations for gas-phase fluid mechanics, heat transfer, thermal radiation and scalar transport are solved in an Eulerian framework. The governing equations for particle-phase mechanics are solved in a Lagrangian reference frame. The overall solution scheme is based on a particle-in-cell approach (Crowe et al, 1977).

Gas properties are determined through local mixing calculations and are assumed to fluctuate randomly according to a statistical probability density function (PDF) characteristic of the turbulence. Turbulence is typically modeled with a two-equation k- ϵ model (Launder and Spaulding, 1972). Gas-phase reactions are assumed to be limited by mixing rates for the major species (local chemical equilibrium) as opposed to chemical kinetic rates for kinetically limited species such as oxides of nitrogen.

Particle mechanics are computed by following the mean path for a discretized group of particles, or particle cloud, in a Lagrangian reference frame. Particle reaction processes include coal devolatilization, char oxidation, and gas-particle interchange. The dispersion of the particle cloud is based on statistics gathered from the turbulent flow field. Heat, mass, and momentum transfer effects are included for each particle cloud. Properties of particles within each cloud are assumed to be uniform. The properties of the local gas field are computed through an ensemble averaging procedure over the extent of the cloud. Particle mass, momentum, and energy sources are converted from a Lagrangian to an Eulerian reference frame by considering the residence time of each particle cloud within the computational cells.

The radiative intensity field and surface heat fluxes are calculated using a discrete ordinates method. Effects of variable surface properties and participating media (gas, soot and particles) are included.

The rates governing the formation and destruction of NO_x are significantly slower than those governing the primary heat release reactions, so the assumption that these species are in local chemical equilibrium leads to inaccurate predictions of their local concentrations. To account for the finite-rate of formation/destruction of these species, additional rate equations are solved. The NO_x chemistry has a negligible effect on the local temperature and velocity fields; hence this analysis is de-coupled from the solution of the turbulent flow field and performed as a "post-process" for computational efficiency.

Computing full finite-rate chemistry for all intermediate species in the NO_x reactions in a turbulent coal or gas fired furnace or boiler is beyond the capability of current combustion simulation tools. However, to obtain engineering estimates of the sensitivity of outlet NO_x to design and operating variables in an industrial combustion system, this degree of detail within the model is not required. This objective can be met through the use of reduced descriptions of the chemical kinetics as long as all other physical mechanisms of first-order importance are also included in the analysis. The effects of both turbulence and finite-rate chemistry are important in obtaining reasonable values for the mean concentrations of NO_x in coal and gas flames (Smoot and Smith, 1985). The NO_x model used in these studies incorporates aspects of both.

OPPOSED WALL-FIRED BOILER OFA STUDY

CFD modeling was used to provide a conceptual design and to evaluate NO_x reduction performance of an overfire air (OFA) system in a 265 MWg B&W, subcritical, opposed-wall, pulverized coal furnace. The furnace is fitted with eighteen Babcock Borsig Power CCV low NO_x burners and baseline NO_x emissions are approximately 0.6 lb/MMBtu. It was expected that OFA ports would be installed on both the furnace front and rear walls. An elevation approximately ten feet above the top burners was suggested for OFA ports; this would provide adequate residence time above the ports for completion of combustion. Making use of symmetry, a 650,000 computational cell half-furnace model was developed. Basic features of the model are shown in Figure 2. Only three of the six front wall burners (for the half furnace model) are opposed by rear wall burners.

The goal of the CFD modeling study was the optimization of the overall OFA system design to maximize the reduction in furnace NO_x emission while minimizing adverse effects such as increased CO emission and increased carbon in fly ash. OFA system design considerations were the horizontal plane OFA port placement, port geometry, air jet velocity, appropriate burner size adjustments, and the level of furnace staging. Before beginning modeling evaluations, AEP Service Corporation engineers worked with modeling engineers to identify feasible locations for the OFA ports on the unit.

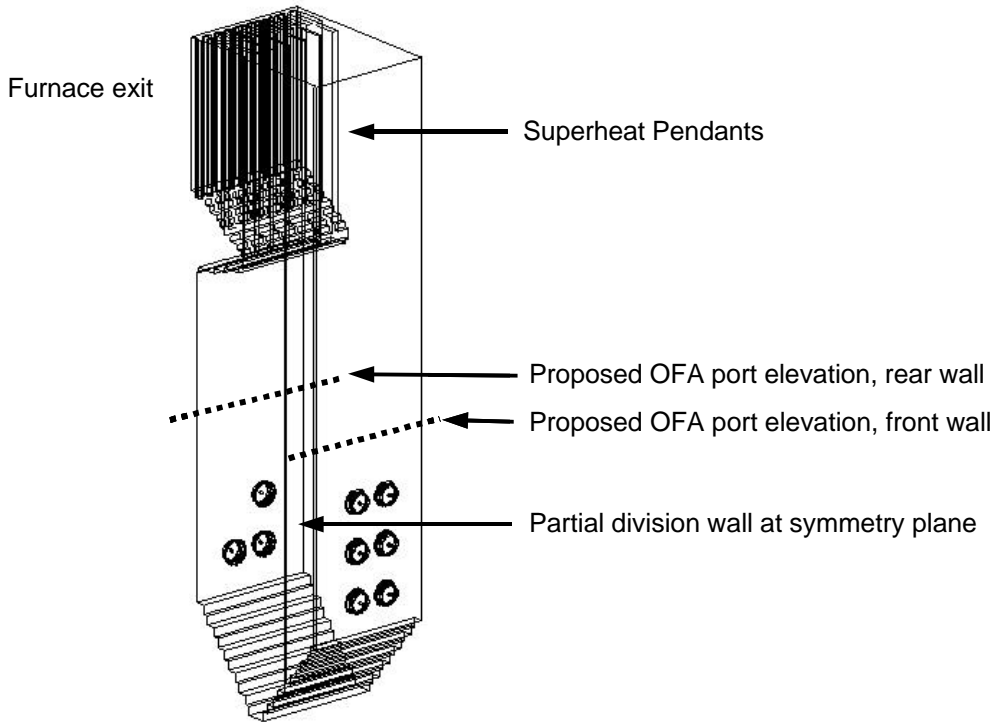


Figure 2. Schematic of half furnace model for opposed wall fired boiler showing OFA port elevations.

Baseline Simulation

An initial baseline simulation was performed to model the current operating condition and to verify the accuracy of the model. The baseline simulation predicted a furnace full load NO_x emission of 0.58 lb/MMBtu, unburned carbon in fly ash (UBC) of 8%, and a model exit CO of 85 ppm. The CO level can be expected to decrease as it moves through the convective pass. With the exception of the unburned carbon level, which was a few percent higher than plant measurements, these values were in line with observed furnace operation.

To evaluate placement of OFA ports in the horizontal plane ten feet above top burners, AEP Service Corporation engineering considered the baseline CO concentration and upward flue gas flow. If the CO and flue gas flow fields are not uniform at this elevation, OFA air will be most effective if concentrated in higher CO and flue gas mass flow regions. Although not considered here, in some cases effective distribution of OFA is provided by a combination of port location as well as biased air flow rates through the ports. The placement of the ports was instead used to effectively bias the OFA distribution in this case study.

Figure 3 shows the location of high CO concentrations and upward flue gas mass flux at the proposed OFA port elevation ten feet above top burners. High CO is present near the rear wall and near the furnace center. The two lobes nearest the front wall come from the top front wall burners below. The upward flue gas flow is highest in the rear half of the furnace, at least partially since there are no upper rear wall burners opposing the upper front wall burners. In the region above the upper front wall burners, the burner swirl results in downward mass flow at this elevation. Although the flow field shown in Figure 3 is for an unstaged furnace and could be

expected to change somewhat with furnace staging, it provides a reasonable basis for locating OFA ports.

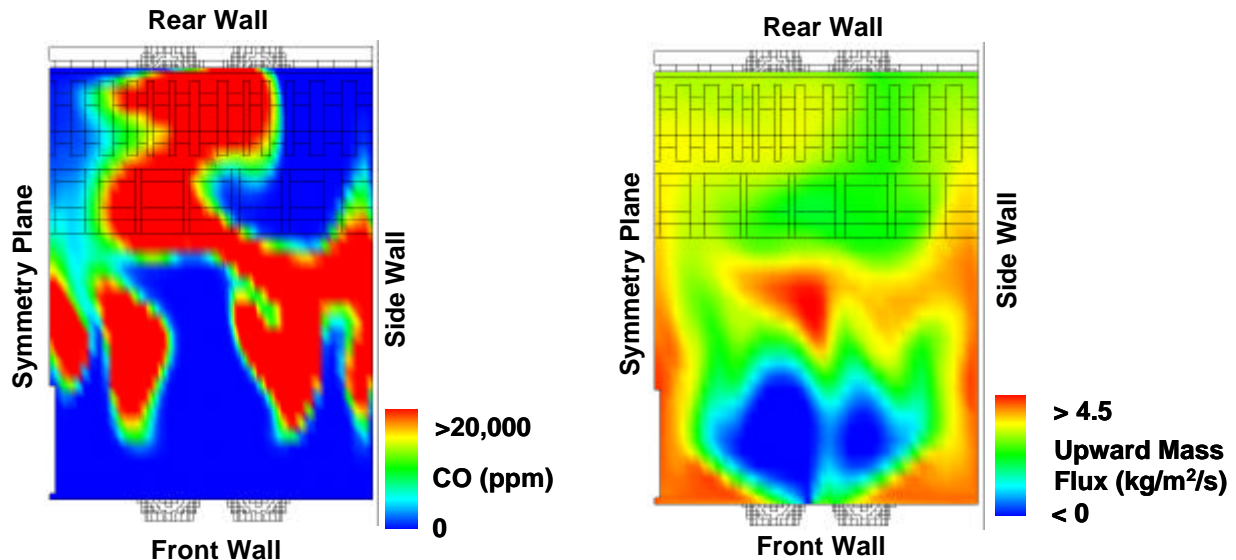


Figure 3. Plots of CO concentrations (left) and upward flue gas mass flux (right) at proposed OFA elevation.

OFA Design and Burner Alterations

Based on the predicted flow field information above, AEP Service Corporation engineers determined a preliminary OFA port layout. The preliminary design is shown in Figure 4. Since high CO regions are nearer the rear wall than the front wall and the upward mass flow is higher in the rear half of the furnace than in the front half, more ports were located on the rear wall than on the front. In addition, it was felt that no OFA port was necessary in the center of the front wall where the predicted flue gas flow is downward, as this would result in the introduction of oxygen rich air into the burner zone. Ports were sized for an OFA jet velocity of 170 ft/s with the lower furnace staged to 0.9. Interlaced ports as in Figure 4 rather than directly opposed OFA jets often help penetration.

Babcock Borsig Power recommends a specific secondary to primary burner air velocity ratio for the CCV burners in this furnace, so with some secondary burner air diverted to the OFA ports, burner modifications were included in the model. To achieve the desired secondary/primary burner air velocity ratio, diameters of the primary coal pipe and secondary air inlet were altered. A summary of predicted results for the baseline and initial OFA cases is shown in Table 1. Key parameters included are the level of furnace staging in the burner zone, burner modifications made to retain recommended fuel and air velocity ratios, and predicted NO_x, UBC and CO concentrations. NO_x reductions over 30% were predicted with OFA, but UBC and CO concentrations also increased significantly. Note that the NO_x, UBC and CO concentrations are at the exit of the computational model, approximately after the first section of superheat pendants and directly above the rear wall of the radiant furnace. NO_x concentrations will not change much beyond this point due to low flue gas temperatures, unburned carbon can decrease slightly, but CO concentrations can be expected to decrease significantly through the back pass of the boiler.

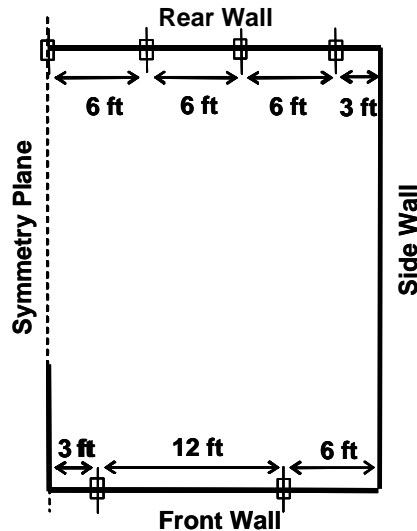


Figure 4. Schematic of proposed OFA port locations on front and rear walls.

A second OFA simulation was performed in order to find a configuration that would produce less of an increase in carbon in fly ash. In the second OFA configuration, the level of furnace staging was decreased to a stoichiometric ratio of 0.95 (vs. 0.90 in the initial OFA simulation). This time only the primary burner diameter was altered to maintain the recommended secondary to primary air velocity ratio and the OFA ports were downsized to maintain a velocity of 170 ft/s. Predicted NO_x remained low (0.38 lb/MMBtu) but the predicted increase in carbon in fly ash was more moderate (now 13% up from 8% in the baseline simulation). Although the simulations indicated that implementation of this configuration in the actual furnace would result in an increase in unburned carbon, the baseline UBC prediction appeared somewhat high suggesting that the final level could be lower than the prediction also, allowing the UBC to remain within acceptable levels.

Model Results

Results from three CFD simulations of this furnace were used by AEP Service Corporation engineering to choose an appropriate OFA system design to reduced furnace NO_x emissions. An overall summary of the simulations is shown in Table 1. Although NO_x is reduced to the same level for both OFA configurations, the increase in carbon in fly ash is less severe for the revised OFA configuration. The furnace is less deeply staged in the revised OFA configuration, but burner modifications also have some impact on NO_x. Although CO increased for both OFA configurations, much of the CO can be expected to burn to completion in the convective pass.

Comparison with Field Testing

The installation of the OFA design, as modeled, was completed in the Spring of 2002. Although AEP Service Corporation not yet fully optimized the system, the NO_x emission rates are in agreement with the modeling effort and both CO emissions (<50 ppm) and unburned carbon in flyash levels (5-10%) are within acceptable ranges. A comparison of the NO_x emission rates, prior to and after the OFA retrofit is illustrated in Figure 5.

Table 1. Summary of simulation results showing the effect of different OFA designs.

	Baseline	Initial OFA	Revised OFA
Furnace Staging	None	0.90	0.95
Burner Modifications	None	Primary & Secondary	Primary
Predicted NOx (lb/MMBtu)	0.58	0.39	0.38
Predicted Carbon in Fly Ash	8%	20%	13%
Predicted CO (at furnace exit)	85 ppm	801 ppm	1000 ppm

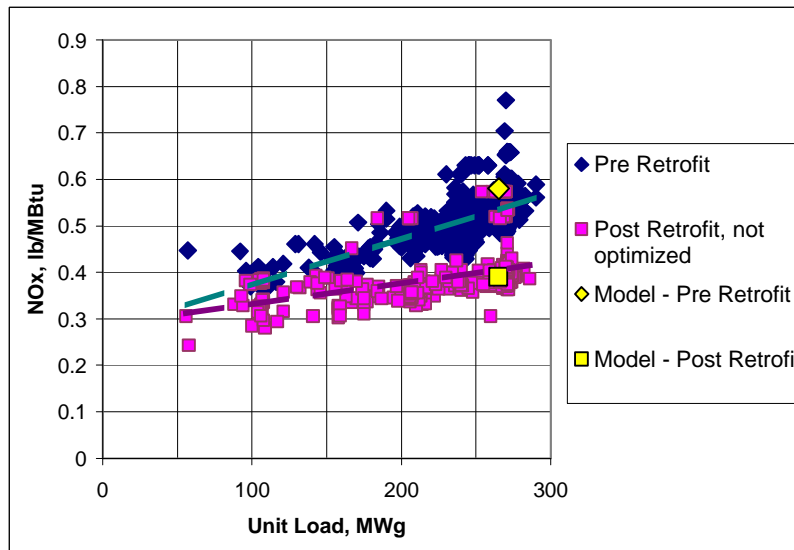


Figure 5. Comparison of predicted and reported NOx emission rates before and after OFA retrofit.

ROOF-FIRED BOILER OFA STUDY

The unit considered in this evaluation is a 150 MW, subcritical, B&W, roof-fired furnace commissioned in 1950. With a symmetry plane at the boiler centerline division wall, a half boiler model consisting of an 800,000 node computational grid was built. An outline of the model and burner details are shown in Figure 6. The half furnace model includes 5 roof mounted multi-tip burners and 5 front wall NOx ports, each aligned vertically with one of the 5 burners. Tube bends in the division wall permit flue gas flow between the two furnace sections.

In the multi-tip burner, also shown in Figure 6, coal and primary air are split into eight tubes of rectangular cross-section arranged in two rows of four tubes each. The tubes extend into the secondary air duct and end at coal tips. Coal and secondary air are fired through six slots

between the roof tubes as shown in the front view of the burner detail. In one furnace configuration modeled in this project, the two outer slots are closed, leaving only the four center slots open. Deflectors mounted over the top and sides the roof tubes divert the coal around the tubes; “flutes” or ridges on the sides of the deflector angle the coal toward the front wall. In each burner, fluted deflectors are used for the forward three pairs of coal tips. The deflector for the rear pair of coal tips is not fluted, so coal from these tips enters the furnace angled toward the rear wall in the direction of the rear coal tubes. Coal and air velocities were specified as inlet conditions to the furnace model at the roof tubes.

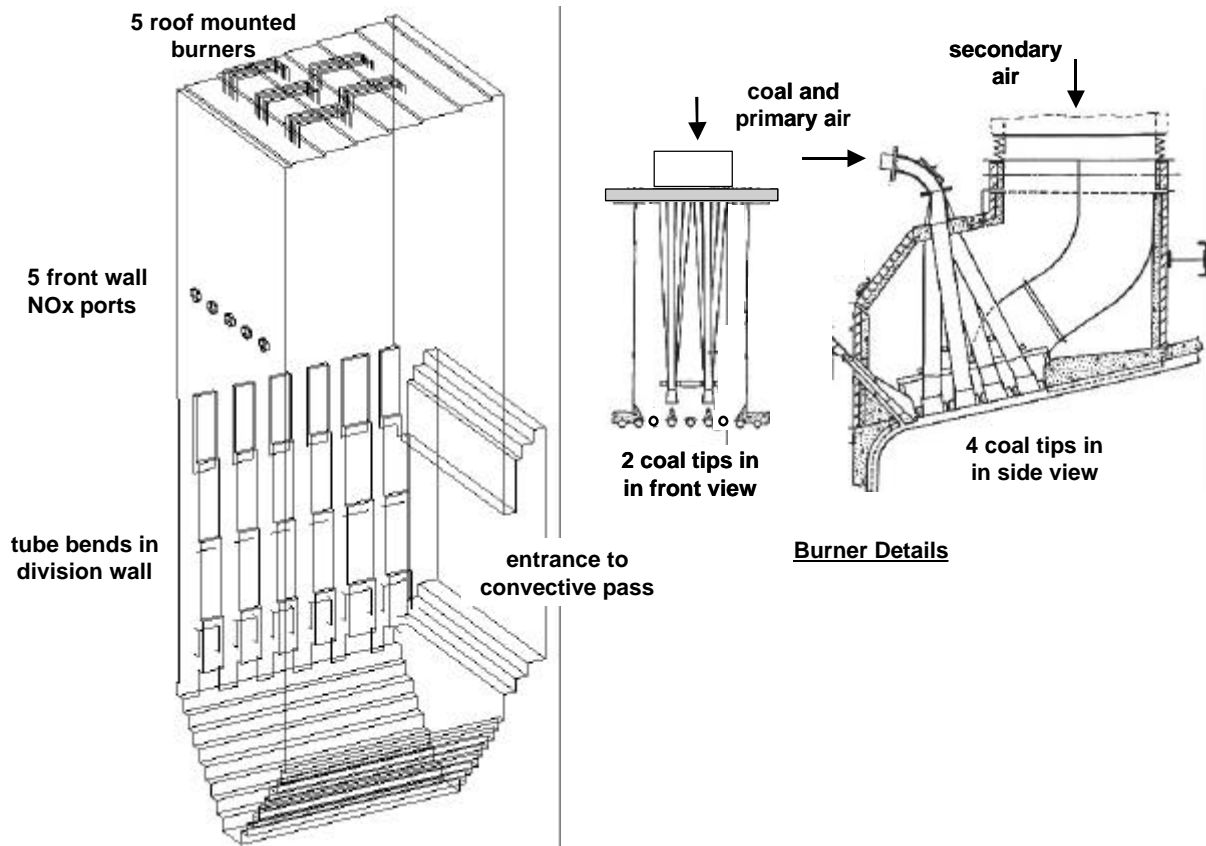


Figure 6. Schematic of the half furnace model and detail of a multi-tip burner from the furnace. In the burner front view, two coal tips fire through six gaps between roof tubes (adapted from Babcock and Wilcox Company, 1963).

Baseline Simulation

A baseline furnace simulation was performed with the furnace at 15% excess air and staged to a burner stoichiometry of 0.84, consistent with the current operating condition. Predictions of the baseline simulation are tabulated in Table 2 and are typical of those currently seen in the furnace. Although CO is high at the furnace exit, it can be expected to decrease substantially in the convective pass entrance region.

Plots of predicted flue gas temperature and CO concentration for the baseline simulation are shown in Figure 7. The vertical temperature plane through the center of the middle front burner shows high temperature and high CO combustion zones below each coal tip. The upper horizontal plane shows distinct high temperature and high CO combustion zones for each burner.

The second horizontal plane shows the reasonably good penetration of the NO_x port jets in the plane of the NO_x ports. In both horizontal planes, high temperature combustion regions are apparent at the interface between the fuel rich primary air/coal streams and the surrounding higher oxygen regions.

The vertical temperature and CO planes Figure 7 show the effect of the flutes on the coal deflectors mentioned earlier. Coal leaving the three front pairs of coal tips encounters fluted deflectors that tend to deflect the coal toward the furnace front wall. However, coal from the rear pair of coal tips encounter deflectors that are not fluted, thus the coal follows the direction of the coal tube toward the furnace rear wall (Figure 6). The direction of the flame from the rear pair of coal tips toward the furnace rear wall is apparent in the vertical planes of Figure 7.

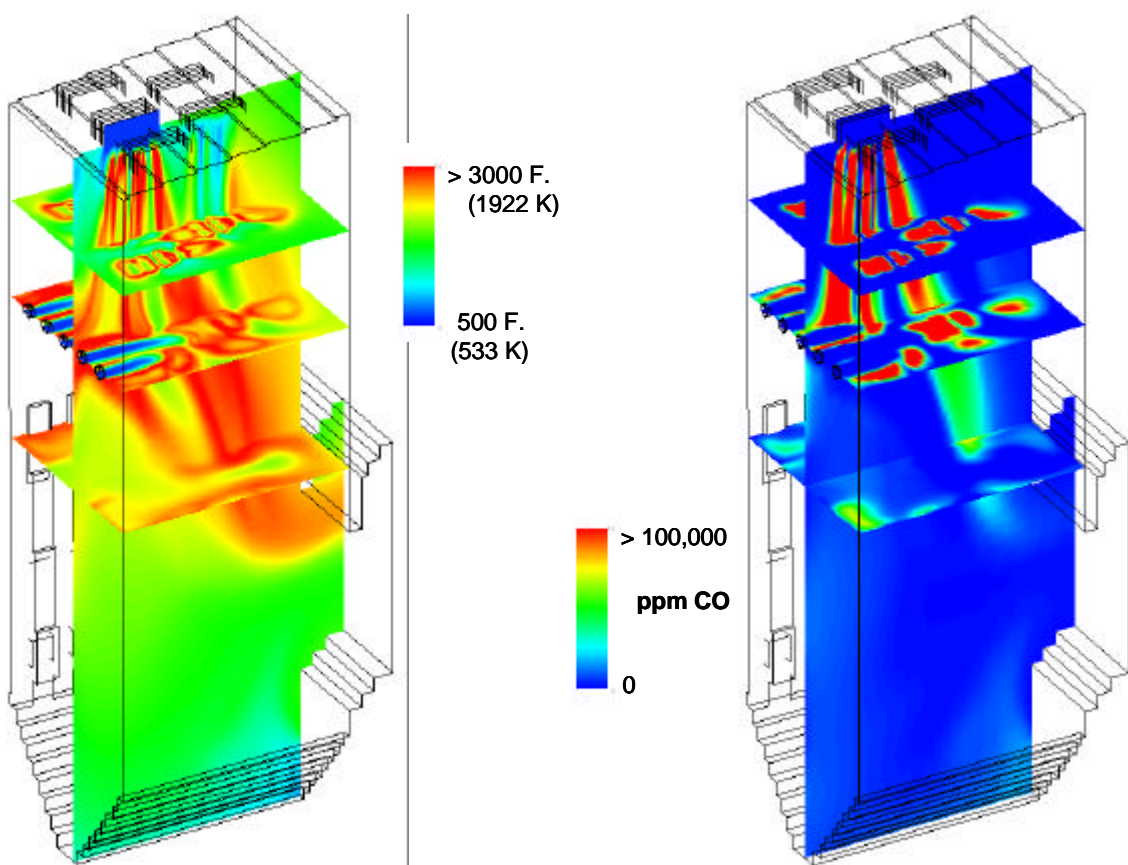


Figure 7. Predicted flue gas temperature and CO concentration for the baseline furnace model.

Predicted Impact of Deeper Staging

In order to reduce furnace NO_x emissions, it was desired to increase furnace staging from the current burner stoichiometry of 0.84. Based on operating experience with other units, an increase in staging to a burner stoichiometry of 0.7 while maintaining overall excess air at 15% was evaluated here. Simulation of this condition predicted a 14% reduction in NO_x emissions and a slight increase in carbon in fly ash. However, operating experience with this unit suggests that the reduction in burner secondary air velocity through diversion of air from the burners to the NO_x ports may increase the propensity for near burner slagging. To maintain a high burner air

velocity and alleviate the possible burner slagging problem, it was suggested that the outer slots between roof tubes for each burner be closed, leaving only the four center slots open. Simulation of this configuration predicted a further decrease in NOx emissions to 23% from the baseline. A summary of the predictions of these simulations compared with the baseline are shown in Table 2. Deeper staging and burner alterations through closing the outer air slots results in little change in carbon in fly ash, some increase in furnace exit CO, and a slight increase in furnace exit temperature, probably due to a shifting of the combustion zone downstream.

In Figure 7 it was noted that the flame from the rearmost pair of coal is directed toward the rear wall and exit of the furnace. This is due to the lack of flutes on the tube deflector associated with this coal tip. Coal from this tip may exit the furnace quickly and thus may not oxidize completely due to a shorter furnace residence time. An analysis of predicted carbon in fly ash for each pair of coal tips is shown in Figure 8. As expected, carbon in fly ash is higher for coal originating from the rear pair of coal tips in each burner. Based on this analysis, it was advised that fluted deflectors be added to the rear pair of coal tips.

Table 2. Summary of Inputs and Predictions

	Baseline	Deeply Staged	Staged and Slots Closed
Burner Stoichiometry	0.84	0.70	0.70
NOx Change from Baseline	-	-14%	-23%
Carbon in Fly Ash	6.9%	8.6%	7.4%
Furnace Exit CO	2750 ppm	2150 ppm	3300 ppm
Furnace Exit Temperature	2352 F.	2379 F.	2379 F.

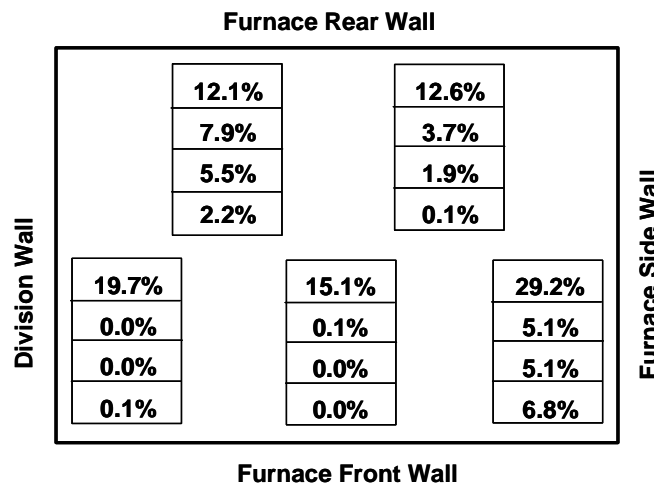


Figure 8. Predicted carbon in fly ash for coal originating from each of the four pairs of coal tips in each of the five burners in the half furnace model.

Predicted Impacts of Water Injection

Water injection was investigated to determine the potential for additional NO_x reduction under deeply staged conditions. AEP has successfully implemented water injection for incremental NO_x reductions in a number of units. The latent heat of vaporization lowers peak flue gas temperatures, which decreases thermal NO_x formation rates. However, a poorly designed water injection strategy can negatively impact furnace efficiency and/or have no impact on NO_x emissions. Since NO_x formed early in the primary combustion zone may be subsequently destroyed, and since lowering combustion temperatures can also decrease NO_x destruction rates, our strategy was to use water injection to attack the downstream thermal NO_x formation regions.

Figure 9 shows plots of the predicted downward flow of NO_x in the furnace vs. distance from the burner for the baseline and deeply staged simulations and the predicted average thermal NO_x formation rate vs. distance from the furnace side wall at the NO_x port elevation. In the downward NO_x flow plot of Figure 9, NO_x production is high in the primary combustion zone near the roof-mounted burners. The increase in this region is less pronounced for the deeply staged simulation due to the decreased availability of oxygen. Between the near burner high NO_x production zone and the NO_x port elevation, NO_x flow levels off and even begins to decrease in the simulation of deeply staged conditions. However, with the introduction of NO_x port air into hot, fuel rich combustion gases, there is an increase in NO_x. The increase is somewhat more pronounced in the simulation of deeply staged conditions.

The plot of thermal NO_x rate vs. distance from the side wall of Figure 9 shows that thermal NO_x formation rates peak between the burners. Since the burner locations coincide with the NO_x ports, the peak thermal NO_x formation zones also lie between the NO_x ports where the cool, oxygen rich jets interact with higher temperature, fuel rich regions.

In order to reduce the thermal NO_x formed between the NO_x ports, a strategy for water injection was devised with six nozzles located a few feet above the NO_x ports and horizontally centered between them. Simulations of three nozzle types were performed: 1) 500 μm volume mean diameter droplets at 5 gpm, 2) 650 μm volume mean diameter droplets at 3 gpm, and 3) 950 μm volume mean diameter droplets at 5 gpm, which reflect flow characteristics of typical “off the shelf”, pressure atomized nozzles. In each case, a distribution of drop sizes with the specified volume mean diameter was used. To attempt to maintain furnace exit temperature, the heat rate was increased by 3% for the 5 gpm cases and by 1.8% for the 3 gpm nozzle.

Water drop trajectories for drops of two initial diameters, 350 μm and 700 μm, are shown Figure 10. The various size droplets in a size distribution will have somewhat different trajectories and Figure 10 shows only two specific sizes within a distribution. Drops with an initial diameter of 700 μm persist longer than the smaller 350 μm initial diameter drops; the 350 μm drops tend to evaporate completely in the vicinity of the NO_x ports. In both cases, drops originating from the center four nozzles are to some degree entrained by the NO_x port jets and probably help to cool the high thermal NO_x formation zones. The entrainment by the NO_x port jets is more pronounced for the smaller drops. Drops originating from the two outer nozzles, however, are trapped in the two front corners and largely miss the high thermal NO_x formation zones.

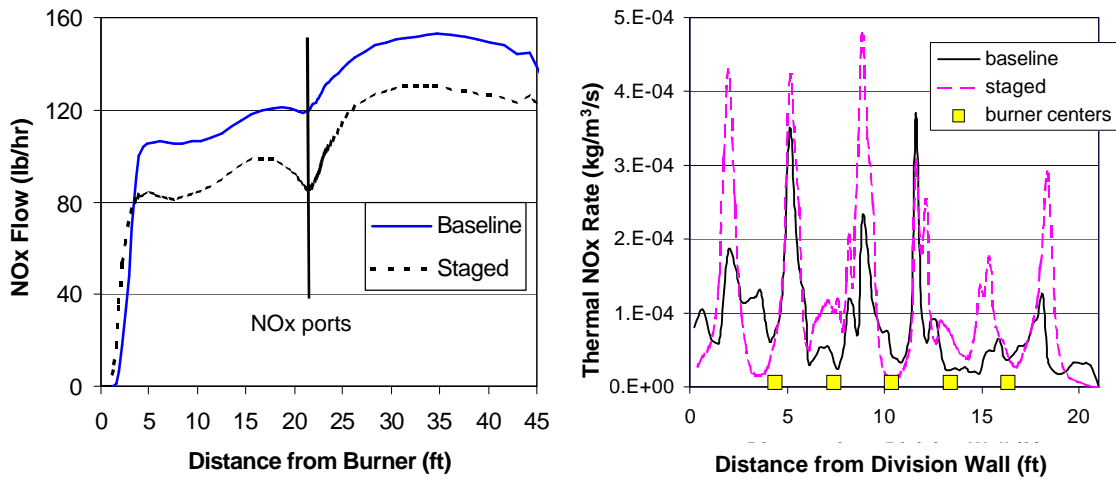


Figure 9. Plots of predicted downward NOx flow vs. distance below the burners (left) and predicted thermal NOx formation rate vs. distance from the furnace side wall at the NOx port elevation (right).

A summary of inputs and NOx predictions for the simulations discussed here is shown in Table 3. The simulations predict that the combination of burner alterations (closing of the outer secondary air slots between roof tubes) and increased burner staging (from a burner stoichiometry of 0.84 to a stoichiometry of 0.70) decreases furnace NOx by 23%. Adding water injection to the more deeply staged furnace is predicted to decrease NOx by up to 37% from the baseline level. The largest NOx reduction is achieved with a total water injection of 30 gpm and 500 μm mean diameter drops. However, this is only a slightly better reduction than the other two water injection configurations. The water injection simulation predicts a decrease in furnace exit CO and a slight increase in carbon in flay ash relative to the deeply staged configuration. The decrease in furnace exit CO with water injection appears to be the result of improved flue gas mixing due to a combination of water spray momentum transfer and increased burner zone turbulence resulting from the increased heat rate. Water injection also results in a decrease in predicted furnace exit temperature in spite of the increased heat rate. The impact on furnace exit temperature is less at the lower rate of water injection.

Since water injection negatively impacts furnace efficiency, it is advantageous to use a low rate of injection to achieve a specific NOx reduction. In this case, injection rates of 18 gpm and 30 gpm of different size distributions achieved the same NOx reduction. Larger diameter drops are slower to evaporate than smaller drops, so the reduced temperature regions will be different.

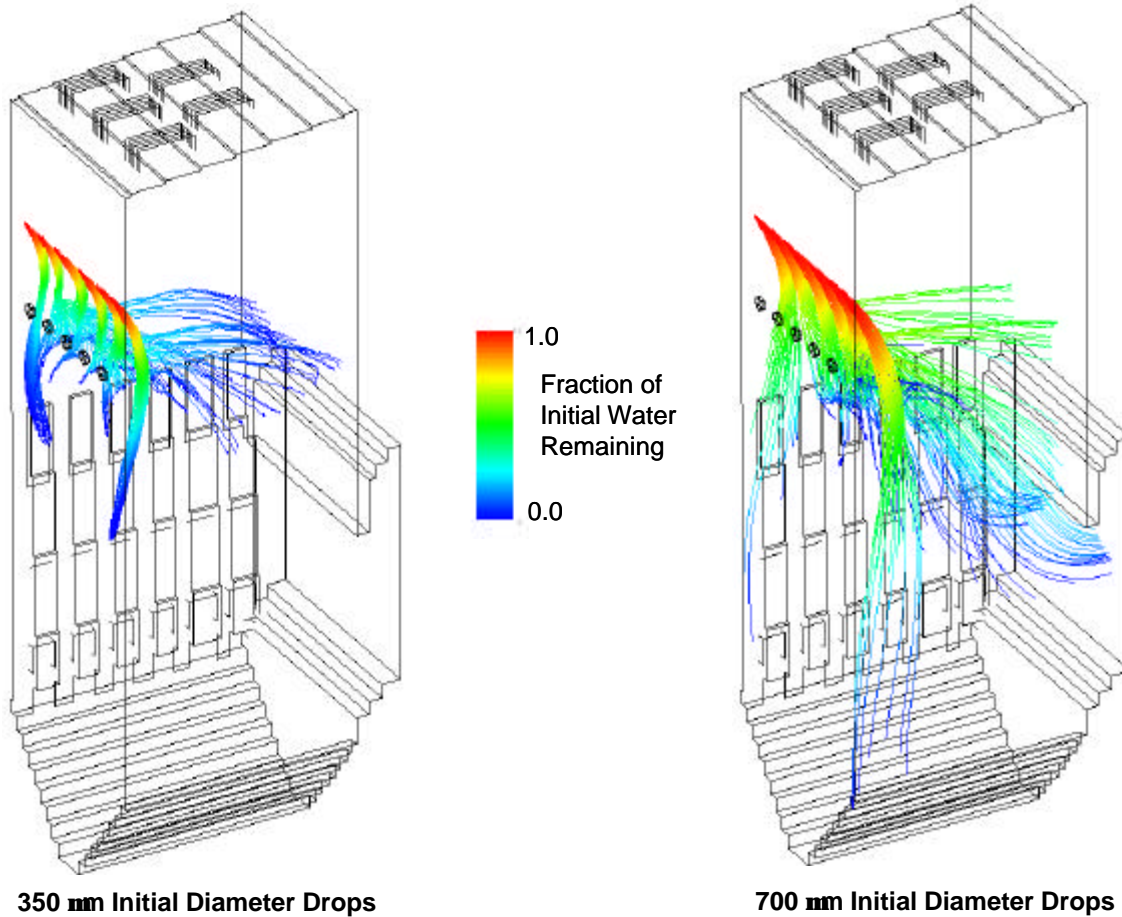


Figure 10. Predicted water droplet trajectories for 350 mm and 700 mm initial diameter drops.

Table 3. Summary of Inputs and Predictions

	Baseline	Deeply Staged	500 mm Dia. Drops	650 mm Dia. Drops	950 mm Dia. Drops
Burner Stoichiometry	0.84	0.70	0.70	0.70	0.70
Total Water Injection Rate	-	-	30 gpm	18 gpm	30 gpm
Heat Rate Change	-	-	+3.0%	+1.8%	+3.0%
NOx Change from Baseline	-	-23%	-37%	-34%	-34%
Carbon in Fly Ash	6.9%	7.4%	9.1%	8.5%	8.8%
Furnace Exit CO	2750 ppm	3300 ppm	2800 ppm	2500 ppm	2200 ppm
Furnace Exit Temperature	2352 F.	2379 F.	2308 F.	2339 F.	2308 F.

Figure 11 shows plots of the cumulative fraction of injected water evaporated (right) vs. distance from the burners and the downward mass flow of NO_x vs. distance from the burners (left). For these simulations, it is desirable for much of the injected water to evaporate in the region of the NO_x ports or just below, where thermal NO_x formation rates are high. The plot of water evaporation in Figure 11 indicates that approximately 40% the total water of the smallest size drop distribution with a mean diameter of 500 μm has evaporated by the time it reaches the NO_x ports. Less of the water in the larger drop sizes evaporates by this time. In this application, the smaller size drop distribution is more optimal for NO_x reduction. However, although for the two extreme cases the cumulative fraction of water evaporated when the NO_x ports are reached varies from approximately 10% to approximately 40%, there is a relatively small impact on NO_x reduction (34% reduction vs. 37% reduction). These results indicate that most of the reduction in NO_x emissions can be achieved with a fairly low rate of water evaporation in the NO_x port region. Nozzles operating at 5 gpm provide little benefit over those operating at 3 gpm, but have a negative impact on furnace efficiency. These simulations simply evaluated the effectiveness of three “off the shelf” nozzles; there was not a concerted effort to determine the characteristics of an optimal nozzle.

The plot of downward mass flow of NO_x in Figure 11 shows that at the NO_x port elevation, NO_x levels are identical for each of the simulations. However, in the region immediately below the NO_x ports, there is an increase in NO_x. The increase in NO_x is mitigated by water injection with the greatest effect in the simulation 500 μm volume average diameter spray.

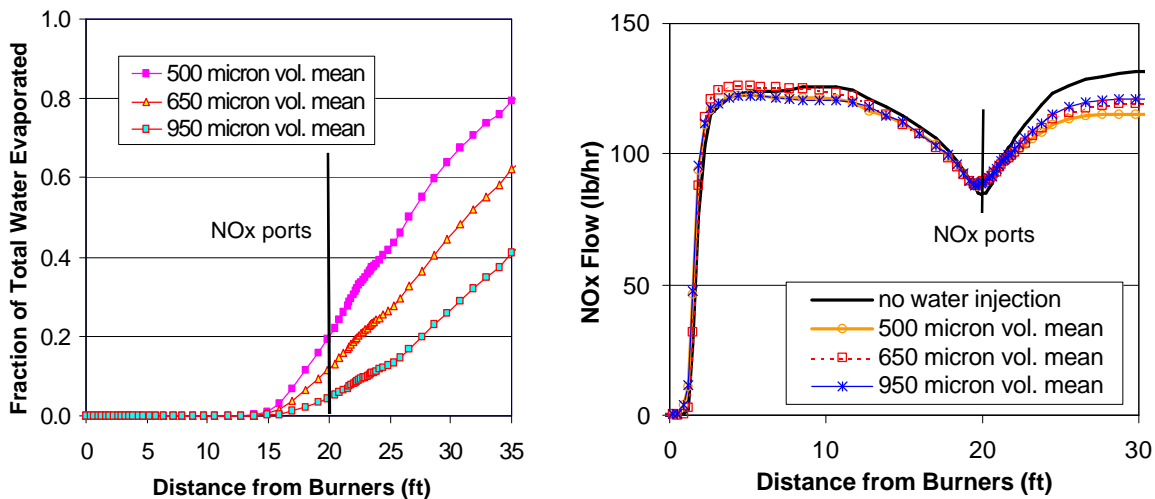


Figure 11. Plots of the cumulative fraction of injected water evaporated (left) and downward NO_x flow (right) vs. distance below the burners.

Comparison with Field Testing

At the time of this writing, burner alterations incorporating the closing of the outer burner slots had been completed. Preliminary test results have shown that combined with deeper staging to a burner SR of approximately 0.7, NO_x reductions of approximately 25% are obtained. This compares with the predicted decrease of 23%. Preliminary indications also are that the NO_x reductions are accompanied by no significant change to stack CO emissions.

CONCLUSIONS

Two examples have been cited to illustrate the approach and effectiveness of using CFD in the design and implementation of the overfire air NO_x reduction technology in coal-fired utility boilers. Both studies were conducted using REI's in-house CFD software specifically developed to account for all relevant combustion processes during coal combustion, including the formation and destruction of nitrogen oxides.

CFD simulations of a 265 MW_g B&W opposed-wall fired pulverized coal furnace fitted with Babcock Borsig Power CCV low NO_x burners have been used by AEP Service Corporation to identify an OFA system design that will maximize the reduction in furnace NO_x emission while minimizing adverse effects such as increased CO emission and increased carbon in fly ash. Modeling results showed NO_x reductions over 30% could be achieved with either of two OFA designs, one with the boiler operating at a stoichiometric ratio of 0.90, the other at 0.95. Although NO_x is reduced to the same level for both OFA configurations, the increase in carbon in fly ash is less severe for the higher stoichiometric ratio OFA configuration. The furnace is less deeply staged in this case, but burner modifications also have some impact on NO_x and appear to compensate for the difference in furnace staging. Although predicted furnace exit CO increased for both OFA configurations over the baseline, much of this CO has been shown through field data to be oxidized in the boiler convective pass. Field-testing and optimization performed by AEP Service Corporation engineering confirmed the CFD predictions of NO_x reduction.

In a second study, simulations of a 150 B&W roof-fired pulverized coal furnace have been performed to evaluate the effect of increased furnace staging accompanied by burner alterations, and water injection on NO_x emissions, CO, and unburned carbon in the fly ash. Furnace staging was increased from a burner stoichiometry of 0.84 to 0.70 and burners were altered to close the outer secondary air slots. For this configuration, the NO_x emissions were predicted to decrease by 23%. Preliminary plant measurements for the recently tested configuration show a drop in NO_x emissions of approximately 25% with no observed change to furnace exit CO.

The analysis predicted an increase in NO_x levels in vicinity of the NO_x ports and further identified regions of high thermal NO_x formation between the ports. Simulations were performed to investigate the impact of water injection in this region to further reduce thermal NO_x formation. The simulations predict that the combination of deeper furnace staging combined with the burner alterations and water injection can reduce furnace NO_x emissions by approximately 37% with a slight increase in carbon in fly ash and a decrease in CO relative to the current operating condition.

The two examples demonstrate the importance and value of accurate CFD modeling when combined with combustion engineering expertise to successful in-furnace NO_x control designs. The CFD modeling results were shown to be very reliable, and are considered essential to optimal design development.

ACKNOWLEDGMENT

The modeling work described herein was supported by funding from American Electric Power (AEP). The OFA modeling work described herein was supported by funding from American Electric Power (AEP). AEP Service Corporation provided engineering management, technical

direction and optimization of the implemented OFA design. Some of the modeling results presented here for the pc-unit were previously published in an ASME paper (Adams et al., 2002; Valentine et al, 2003) and are used here with permission of ASME.

REFERENCES

- Adams, B., Cremer, M., Valentine, J., Bhamidipati, V., Letcavits, J., O'Connor, D., and Vierstra, S., "Use of CFD Modeling for Design of NO_x Reduction Systems in Utility Boilers," Proceedings of the 2002 International Joint Power Generation Conference, ASME, Phoenix, AZ, June, 2002
- Babcock & Wilcox Company, 1963, *Steam: Its Generation and Use*, Thirty-Seventh Edition, New York, 1963.
- Bockelie, M.J., Adams, B.R., Cremer, M.A., Davis, K.A., Eddings, E.G., Valentine, J.R., Smith, P.J., Heap, M.P., PVP-Vol. 377-2, 1998, "Computational Simulations of Industrial Furnaces," Computational Technologies For Fluid/Thermal/Chemical Systems with Industrial Applications, ASME, pp. 117-124.
- Chen, W., "Modeling of nitrogen pollutants in coal combustion," PhD dissertation, Chemical Engineering Department, Brigham Young University, Provo, UT 1994.
- Crowe, C.T., and Sharma, M.D., and Stock, D.E., 1977, "The Particle-Source-in-Cell (PSI-Cell) Model for Gas-Droplet Flows," *Journal of Fluids Engineering*, 99, pp. 325-332.
- DeSoete, G.G., 1975, "Overall reaction rates of NO and N₂ formation from fuel nitrogen," *Fifteenth Symposium (Int.) on Combustion*, The Combustion Institute, Pittsburgh.
- Launder, B.E., and Spaulding, D.B., 1972, *Mathematical Models of Turbulence*, Academic Press, London.
- Smoot, L.D. and Smith, P.J., 1985, *Coal Combustion and Gasification*, Plenum Press, NY, NY.
- Valentine, J.R., Cremer, M.A., Davis, K.A., Letcavits, J.J., and Vierstra, S.A., "A CFD Model Based Evaluation of Cost Effective NO_x Reduction Strategies in a Roof-Fired Unit," Proceedings of the 2003 International Joint Power Generation Conference, ASME, Atlanta, GA, June, 2003.
- Wendt, J.O.L., 1980. "Fundamental coal combustion mechanisms and pollutant formation in furnaces," *Prog. Energy Combust. Sci.*, Vol. 6, pp. 201-222.